THE JOURNAL OF PHYSICAL CHEMISTRY A
A JOURNAL OF THE AMERICAN CHEMICAL SOCIETY

A Combined Crossed Molecular Beam and Theoretical Investigation of the Elementary Reaction of Tricarbon ($C_3(X^1\Sigma_g^+)$) with Diacetylene ($C_4H_2(X^1\Sigma_g^+)$): Gas Phase Formation of the Heptatriynylidyne Radical (*l*-$C_7H(X^2\Pi)$)

Iakov A. Medvedkov, Anatoliy A. Nikolayev, Zhenghai Yang, Shane J. Goettl, Alina A. Kuznetsova, André K. Eckhardt, Alexander M. Mebel,* and Ralf I. Kaiser*

Cite This: *J. Phys. Chem. A* 2025, 129, 3931−3939

ABSTRACT: An elucidation of the underlying formation pathways to acyclic hydrocarbons such as polyynes (C_nH_2), cumulenes (C_nH_2), and linear resonantly stabilized linear radicals (*l*-C_nH) is indispensable to understand the hydrocarbon chemistry in extreme low- and high-temperature environments. In this study, we exploited the crossed molecular beam technique to investigate the reaction of tricarbon $C_3(X^1\Sigma_g^+)$ with diacetylene (butadiyne; HCCCCH; $X^1\Sigma_g^+$) at a collision energy of 47 ± 1 kJ mol^{-1}. The experimental data were merged with *ab initio* calculations of the singlet C_7H_2 potential energy surface (PES) revealing that the reaction is initiated via the formation of an initial van der Waals reactant complex in the entrance channel. Subsequent rearrangements lead to various carbene-type and cyclic intermediates via ring-opening, ring-closure, and hydrogen migration processes, eventually forming acyclic C_7H_2 isomers prior to their barrierless unimolecular decomposition to the most stable linear isomer, heptatriynylidyne (C_7H, $X^2\Pi$) in an overall endoergic reaction (+57 kJ mol^{-1}). The reaction exhibits strong similarities to the tricarbon−acetylene (C_3−C_2H_2). The significant energy threshold suggests that the tricarbon reaction with (poly)acetylenes forming resonantly stabilized linear radicals is open in high-temperature environments such as combustion flames and circumstellar envelopes of carbon stars and planetary nebulae as their descendants; however, these reactions are closed in low-temperature environments as in cold molecular clouds and hydrocarbon-rich atmospheres of planets and their moons such as in Titan.

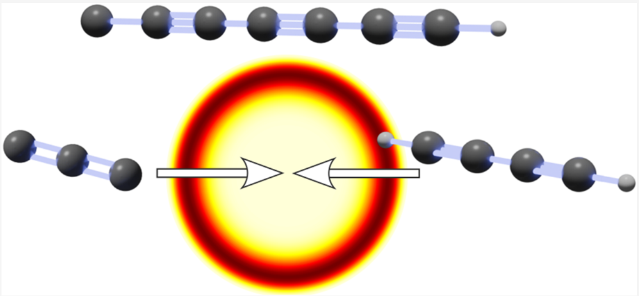

1. INTRODUCTION

Hydrogen-deficient resonance stabilized free radicals (RSFRs) are vital for the synthesis and growth of polycyclic aromatic hydrocarbons (PAH) and the production of soot and carbonaceous particles in combustion flames,[1−6] extraterrestrial environments,[7−14] and chemical vapor deposition systems (CVD).[15] Since RSFRs are produced as transients *in situ*, the pathways of their production hold critical insight into the comprehension of molecular mass growth processes and aromatization processes. From a chemical bonding point of view, feasible ways of producing hydrocarbon RSFR in high- and low-temperature environments can be divided into two groups. The first group encompasses those processes that require bond ruptures in closed-shell molecules: a carbon−hydrogen (C−H) bond rupture, direct hydrogen atom abstraction, carbon−carbon (C−C) *β*-scission, and photolysis. The second group categorizes processes that require the formation of at least one new chemical bond en route to the generation of RSFRs. The most eloquent examples of this class are reactions of atomic carbon (C), dicarbon (C_2), and tricarbon (C_3) with unsaturated hydrocarbons, which eventually result in larger hydrogen-deficient hydrocarbon radicals, in particular RSFRs, after unimolecular decomposition of the reaction intermediates.[8,11,16−18] Since bare carbon clusters have been detected in high-temperature combustion flames,[19] in circumstellar envelopes of carbon-rich asymptotic giant branch stars (AGBs),[20] and in CVD processes[15] leading to diamonds, their reactions with hydrocarbons yield chemical information vital to demystifying molecular mass growth mechanisms in these systems. Extensive theoretical and crossed molecular beam studies have been performed for C(^3P),[8,9,16,21−24] $C_2(X^1\Sigma_g^+/a^3\Pi_u)$,[17,25−34] and $C_3(X^1\Sigma_g^+)$[18,35,36] with key classes of unsaturated hydrocarbons leading to

Received: February 27, 2025
Revised: April 12, 2025
Accepted: April 15, 2025
Published: April 22, 2025

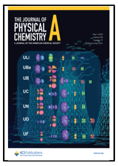

https://doi.org/10.1021/acs.jpca.5c01330

RSFRs. Notably, reactions of unsaturated hydrocarbons with $C(^3P)$ and $C_2(X^1\Sigma_g^+/a^3\Pi_u)$ were found to have no entrance barrier and form RSFRs in overall exoergic reactions. This opens those elementary reactions even in the low-temperature environments,[8−11,18] while reactions with $C_3(X^1\Sigma_g^+)$ reveal opposite features, entrance barrier of 30−50 kJ mol^{-1} and endoergicities of up to 100 kJ mol^{-1}.[10,11,18]

Considering that hydrogen-deficient, acyclic hydrocarbons such as polyynes (C_nH_2), cumulenes (C_nH_2), and linear RSFRs (l-C_nH) with up to ten carbon atoms may account for up to 40% of the interstellar carbon budget,[37,38] an elucidation of the underlying formation pathways is instrumental to understand the hydrocarbon chemistry in extreme low- and high-temperature environments.[11,18,35] Reactions of carbon atoms[39] and dicarbon[27] with the first representative of the polyyne series—diacetylene (C_4H_2)—were studied in detail. However, the reaction of tricarbon $C_3(X^1\Sigma_g^+)$ with diacetylene (C_4H_2) has not yet been probed experimentally yet. The potential output of this reaction is the formation of heptatriynylidyne radical (C_7H), which was first observed in a laboratory in 1996[40,41] in acetylene-argon discharge via rotational spectroscopy recording rotational transitions in the ground $^2\Pi_{1/2}$ state and in the $^2\Pi_{3/2}$ state (37 K higher in energy). Based on this data, C_7H was then detected in IRAM 30 m telescope observations of IRC + 10216 with an estimated column density of ~2×10^{12} cm^{-2}.[42] The subsequent survey of the heptatriynylidyne radical in the TMC-1 using NRAO6 43 m telescope did not find this species within the cold molecular cloud.[43]

Here, by utilizing the crossed molecular beam experiments augmented by high-level quantum chemistry, we reveal that the heptatriynylidyne radical (C_7H, $X^2\Pi$) can be prepared in the gas phase under single-collision conditions via the reaction of tricarbon (C_3; $X^1\Sigma_g^+$) with diacetylene (HCCCCH; $X^1\Sigma_g^+$). This reaction commences with the formation of an initial van der Waals complex in the entrance channel. Subsequent rearrangements lead to various carbene-type and cyclic intermediates via ring-opening, ring-closing, and hydrogen migration processes, eventually forming acyclic C_7H_2 isomers prior to their barrierless unimolecular decomposition to the most stable linear isomer, heptatriynylidyne (C_7H, $X^2\Pi$) in an overall endoergic reaction (+57 kJ mol^{-1}). While this threshold energy prohibits this elementary reaction from playing any role in low-temperature environments, high-temperature environments like combustion flames and circumstellar envelopes of carbon stars as of IRC+102161 may facilitate the gas phase formation of the heptatriynylidyne radical (C_7H, $X^2\Pi$).

2. EXPERIMENTAL AND COMPUTATIONAL SECTION

2.1. Crossed Molecular Beam Experiment.

The gas phase reaction of the tricarbon (C_3; $X^1\Sigma_g^+$) with diacetylene (butadiyne; HCCCCH; $X^1\Sigma_g^+$) was carried out under single-collision conditions using the crossed molecular beams machine.[14,44] The experimental setup, data acquisition, and data processing have been discussed previously;[35,45−47] here, we will only provide a brief summary. A pulsed tricarbon beam (C_3; $X^1\Sigma_g^+$) was generated in the primary source chamber by laser ablation (3 mJ, 266 nm, 30 Hz; quadrupole irradiation) from a rotating and translating graphite rod. The ablated tricarbon was seeded in a pulsed helium beam (He, 99.9999%; Airgas) released from a piezoelectric valve operating at 60 Hz and a backing pressure of 4 atm. A four-slot chopper wheel mounted between the skimmer and the cold shield selected a section out of the seeded tricarbon beam with a peak velocity of $v_p = 1863 \pm 20$ m s^{-1} and speed ratio of $S = 3.8 \pm 0.8$. This segment of the tricarbon beam crossed a pulsed beam of diacetylene (60 Hz, $v_p = 1023 \pm 16$ m s^{-1}, $S = 15.0 \pm 1.2$) seeded at a level of 1% in a 4:1 mixture of helium and argon (He and Ar: 99.9999%, Matheson) at a backing pressure of 1 atm triggered 40 μs prior to the tricarbon beam. Diacetylene is not commercially available and was synthesized by the one-stage method as reported in the literature.[6,48−50] Both molecular beams intersected perpendicularly in the scattering chamber at a mean collision energy of $E_C = 47 \pm 1$ kJ mol^{-1}. The reactively scattered products were monitored by a triply differentially pumped 'universal' detection system[51,52] rotatable in the scattering plane defined by the primary and secondary beams. At the entry of the detector neutral products are ionized by electron ionization (80 eV, 2 mA) before mass separation by a quadrupole mass filter (Extrel, QC 150; 2.1 MHz) and detected by Daly type ion counter.[53] Angularly resolved time-of-flight (TOF) spectra were accumulated at discrete laboratory angles (Θ) in 2.5° steps between 25.25 and 45.25°. Operating the laser at 30 Hz and the pulsed valve at 60 Hz allowed an instant background subtraction ("laser-on" minus "laser-off") during the TOF recording.

Information on the chemical dynamics was obtained by fitting these TOF spectra of the reactively scattered products and the product angular distribution in the laboratory frame (LAB), using a forward-convolution routine.[54,55] This approach uses the trial angular flux $T(\theta)$ and translational energy $P(E_T)$ distributions in the center-of-mass (CM) frame to compute the laboratory data (TOFs and LAD). CM functions were then iteratively varied until the best fit of the TOF spectra and LAD were achieved. Together, the CM functions represent the reactive differential cross section $I(u, \theta) \sim P(u) \times T(\theta)$, where u is the CM velocity, which is represented as a flux contour map, thus depicting an overall image of the reaction outcome. Since the reactions of tricarbon molecules with unsaturated hydrocarbons have characteristic threshold energies (E_0), we utilized an energy-dependent cross section (σ) from collisional energy (E_{coll}), by applying the line-of-center model through eq 1[56,57] in the fitting routine.

$$\sigma \sim \begin{cases} 0, & E_{coll} < E_0 \\ 1 - \dfrac{E_0}{E_{coll}}, & E_{coll} \geq E_0 \end{cases} \tag{1}$$

2.2. Theoretical Calculations.

The long-range corrected hybrid ωB97X-D density functional[58] in conjunction with Pople's split-valence 6-311G(d,p) basis set[59] in the Gaussian 09 software package[60] was initially used to optimize geometries and to compute vibrational frequencies of various stationary structures on the singlet C_7H_2 potential energy surface (PES), such as reactants, products, intermediates, and transition states. The unrestricted open-shell UωB97X-D method was specifically selected for singlet intermediates and transition states to verify which of them have a biradical character judging by a nonzero $\langle S^2 \rangle$ expectation value, meaning that a wave function in open-shell singlet state is not properly described using a single-determinant approach. The structures with biradical character required multireference calculations for refining the relative energy (*vide infra*). The stability of the SCF solution for all of the structures was also checked. The nature of all transition states was confirmed by means of intrinsic reaction coordinate (IRC)[61] calculations at the UωB97X-D/6-311G-(d,p) level of theory.

To improve the accuracy of the DFT relative energies, the explicitly correlated restricted closed-shell coupled clusters RCCSD(T)-F12b[62,63] theory with single and double excitations and the perturbation theory treatment for triple excitations, alongside Dunning's correlation-consistent triple-ζ cc-pVTZ-f12[64] basis set was used for single-point energy calculations in Molpro 2015[65] for the structures with $\langle S^2 \rangle$ = 0.0. However, most of these single-determinant calculations have also confirmed that there is a need for additional multireference calculations even for closed-shell structures, where the T1 diagnostics values exceeded 0.02. For all structures where the single-reference-based CCSD(T)-F12b method was expected to be unreliable, that is, for biradicals and closed-shell singlets with the T1 diagnostics exceeding 0.02, the multireference complete active space second-order perturbation theory (CASPT2) method[66,67] was employed with Dunning's correlation-consistent triple-ζ cc-pVTZ[64] basis set and using initial orbitals from full valence, multireference complete active space self-consistent field (CASSCF) calculations[68,69] with the same basis set. The active space for CASPT2 optimal in terms of the calculation time and proper description of the wave function included all π orbitals and was composed of 12 electrons distributed on 12 orbitals. To combine the CCSD(T)-F12b and CASPT2 energies together on the potential energy diagram, we computed relative CASPT2 energies of various species with respect to the energy of the nearest intermediate $\boldsymbol{i_x}$ on the PES with T1 diagnostics not exceeding 0.02, which means that its wave function can be described with the single-determinant CCSD(T)-F12b method, or the entrance intermediate ***i1***. This allowed us to avoid using the bimolecular reactants as the zero reference energy level and thus to circumvent the issue of the absence of size consistency in the CASPT2 method. In this approach, the final relative energy for the considered stationary point was obtained using the following expression,

$$\begin{aligned} E(\text{rel})_{\text{final}}&(\text{stationary point}) \\ &= E(\text{rel})_{\text{CCSD}(T)-F12b/\text{cc-pVTZ}-F12}(i_x) \\ &\quad + \Delta E_{\text{CASPT2}(12,12)/\text{cc-pVTZ}} \end{aligned}$$

where

$$\begin{aligned} \Delta E&_{\text{CASPT2}(12,12)/\text{cc-pVTZ}} \\ &= E_{\text{CASPT2}(12,12)/\text{cc-pVTZ}}(\text{stationary point}) \\ &\quad - E_{\text{CASPT2}(12,12)/\text{cc-pVTZ}}(i_x) \end{aligned}$$

If the CCSD(T)-F12b/cc-pVTZ-F12 energy for $\boldsymbol{i_x}$ is trustworthy based on the $\langle S^2 \rangle$ and T1 diagnostics values, it is taken as a reference. For each particular structure with a multireference wave function, $\boldsymbol{i_x}$ was chosen as the closest intermediate. Alternatively, the initial intermediate ***i1***, whose wave function does not exhibit a strong multireference character, was taken as the reference in the relative energy calculations. In the meantime, we could not employ the composite triplet-singlet gap method[70,71] to obtain refined relative energies, because almost all CCSD(T)-F12b calculations for triplet states had shown the T1 diagnostics values above 0.025, making their CCSD(T)-F12b/cc-pVTZ-f12 energies unreliable.

The total CCSD(T)-F12b/cc-pVTZ-f12//ωB97X-D/6-311G(d,p) + ZPE[ωB97X-D/6-311G(d,p)] theoretical scheme involving its expansion with the multireference E_{CASPT2}(12,12)/cc-pVTZ approach is expected to provide accuracy within 4 kJ mol^{-1} or even better.[72]

For a supermolecule constituted from noninteracting products ***p1*** + H at large separation, the (12e,12o) active space appeared to be insufficient and hence, the following strategy was used to refine their relative energy. Two CASPT2 calculations were carried out, first, with the active space (16e,16o) for a supermolecule of the reactants and, second, with the active space (15e,15o) for the linear C_7H product ***p1***, with the addition of the exact energy of −0.5 hartree for the hydrogen atom. The reactants' supermolecule, C_3; $X^1\Sigma_g^+$ + HCCCCH; $X^1\Sigma_g^+$, has the closed-shell singlet ground state. Alternatively, the products' supermolecule consisting of doublet fragments had an open-shell singlet wave function resulting in failure of the CASPT2(16,16) calculation at the available supercomputing facilities. Therefore, the relative energy of the C_7H + H products was computed within the following scheme:

$$\begin{aligned} E^{\text{REL}}(p1 + H) &= E_{\text{CASPT2}(15,15)/\text{cc-pVTZ}} + E_{\text{exact}}(H) \\ &\quad - E_{\text{CASPT2}(16,16)/\text{cc-pVTZ}}(C_4H_2 + C_3) \end{aligned}$$

with an assumption that the deviation from size consistency

$$\begin{aligned} E&_{\text{CASPT2}(16,16)/\text{cc-pVTZ}}(p1 + H) \\ &- \{E_{\text{CASPT2}(15,15)/\text{cc-pVTZ}}(p1) + E_{\text{exact}}(H)\} \end{aligned}$$

is small.

3. RESULTS

3.1. Laboratory Frame. The reactive scattering signal for the reaction of the tricarbon (C_3; 36 amu) with diacetylene (HCCCCH; 50 amu) was observed at mass-to-charge ratios m/z = 85 (C_7H^+) suggesting that it originated from the reaction channel forming the C_7H product and atomic hydrogen (reaction 2). No signal was detected at m/z = 84 (C_7^+) advocating that only the tricarbon versus atomic hydrogen reaction to form C_7H radical(s) is open but not the molecular hydrogen elimination channel.

$$\begin{aligned} &C_3\ (36\ \text{amu}) + \text{HCCCCH}\ (50\ \text{amu}) \\ &\quad \rightarrow C_7H\ (85\ \text{amu}) + H\ (1\ \text{amu}) \end{aligned} \tag{2}$$

Hence, m/z = 85 was exploited to collect TOF spectra at discrete intervals in steps of 2.5° from 25.25 to 45.25° Θ (Figure 1). The resulting TOFs were then normalized with respect to the center-of-mass angle of 35.25° to obtain the laboratory angular distribution (Figure 1b). Notable features of the LAD include its width of only 15° and slight asymmetry around the CM angle at 37.3 ± 1.1°. These findings might propose that the C_7H products were formed via indirect scattering dynamics through complex formation involving one or more C_7H_2 reaction intermediates.[8,14,52,56,73−77]

3.2. Center-of-Mass Frame. It should be emphasized that in order to get an acceptable fit of the data, it was necessary to introduce an energy dependence of the reactive cross section via eq 1. The fit with use of reaction cross section proportional to $E_C^{-(1/3)}$ (as in the case of a reaction with no threshold dominated by long-range induced dipole-induced dipole

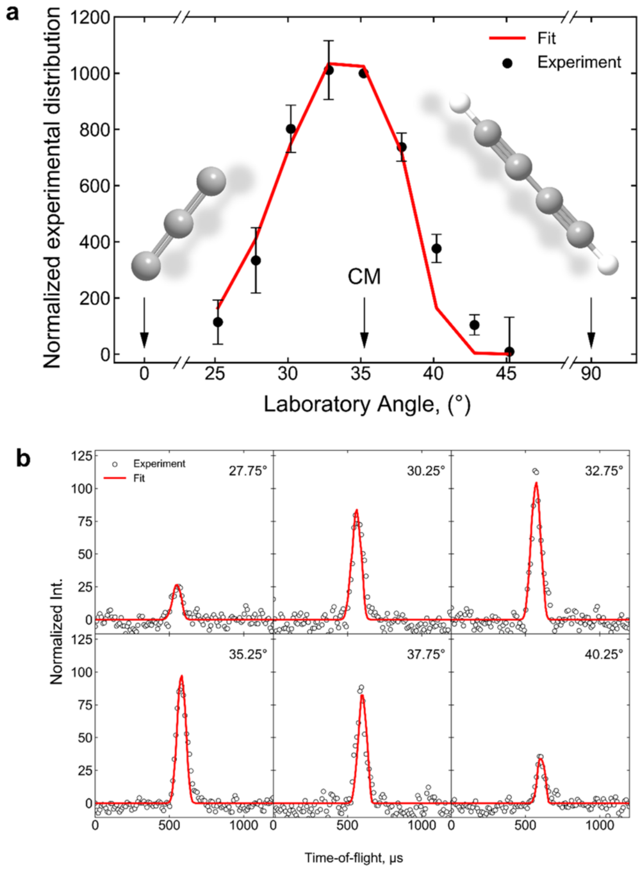

Figure 1. (a) Laboratory angular distribution (b) and time-of-flight (TOF) spectra recorded at m/z = 85 for the reaction of tricarbon $C_3(X^1\Sigma_g^+)$ with diacetylene $C_4H_2(X^1\Sigma_g^+)$ at a collision energy of 47 ± 1 kJ mol^{-1}. The circles represent the experimental data, and the red solid lines are the best fits; the gray atoms are carbon, and the white atoms are hydrogen.

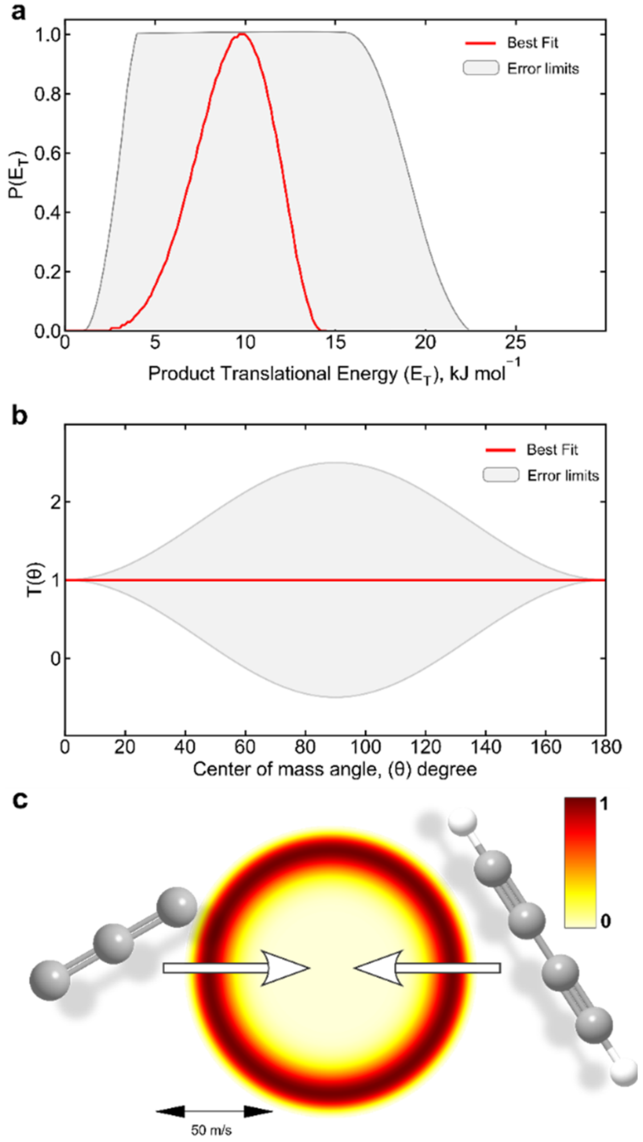

Figure 2. (a) Center-of-mass translational energy $P(E_T)$, (b) angular T(θ) flux distributions, and (c) flux contour map for the reaction of tricarbon $C_3(X^1\Sigma_g^+)$ with diacetylene $C_4H_2(X^1\Sigma_g^+)$. The solid lines represent the best fit, while the shaded areas indicate the error limits. For T(θ), the direction of the tricarbon beam is defined as 0° and of the diacetylene as 180°. The gray atoms are carbon, and the white atoms are hydrogen.

interactions) was unable to replicate the laboratory data (Figures S6 and S7). The best fit for the laboratory data was derived for a single channel (reaction 2) with a threshold energy of 40 kJ mol^{-1}. The best-fit CM functions are depicted in Figure 2 where the gray-filled areas define the limits of the acceptable fits. Considering the translational energy flux distribution $P(E_T)$ (Figure 2a), the maximum energy (E_{max}) portrays the kinetic energy of those molecules born without internal excitation. According to energy conservation, $E_{max} = E_C - \Delta_rG$, where E_C is the mean collision energy and Δ_rG is the reaction energy. The $P(E_T)$ distribution depicts a maximum energy of the acceptable fits of 14 ± 8 kJ mol^{-1} (Figure 2a). Taking into consideration this spread of possible E_{max} and the collision energy of 47 ± 1 kJ mol^{-1}, we can calculate the endoergicity of the reaction Δ_rG to be 33 ± 9 kJ mol^{-1} for the atomic hydrogen loss channel (reaction 2).

Additional information about the reaction dynamics can be obtained from the CM angular distribution $T(\theta)$ (Figure 2b). It should be emphasized that the very narrow range of the reactive scattering signal as evident from the LAB distributions combined with the low speed ratio of the tricarbon beams makes it problematic to derive quantitative information from the center-of-mass angular distributions, $T(\theta)$. Based on the limited speed ratio, the fluctuations of the tricarbon beam velocity, and the narrow range of the reactive scattering signal, the overall fit is not sensitive to exploiting an isotropic/sideways/coplanar distribution. However, the symmetry around 90° and intensity at all angles in all acceptable fits propose indirect scattering dynamics through the formation of C_7H_2 complex(es) and lifetime(s) of intermediates longer than the(ir) rotational period(s).[56] These findings are also supported by the flux contour map (Figure 2c), which shows an overall image of the reaction and scattering process.

4. DISCUSSION

For complex polyatomic systems, it is unavoidable to integrate experimental findings with the electronic structure to reveal the underlying reaction mechanism and the nature of the isomer(s) formed. The computations discovered 20 possible reaction intermediates in form of carbenes (**i1**-**i12**, **i14**, **i16**, **i17**, **i19**, **i20**) and ***singlet*** biradicals (**i13**, **i15**, **i18**) connected by 32 transition states on the singlet PES (Figure 3 and Table

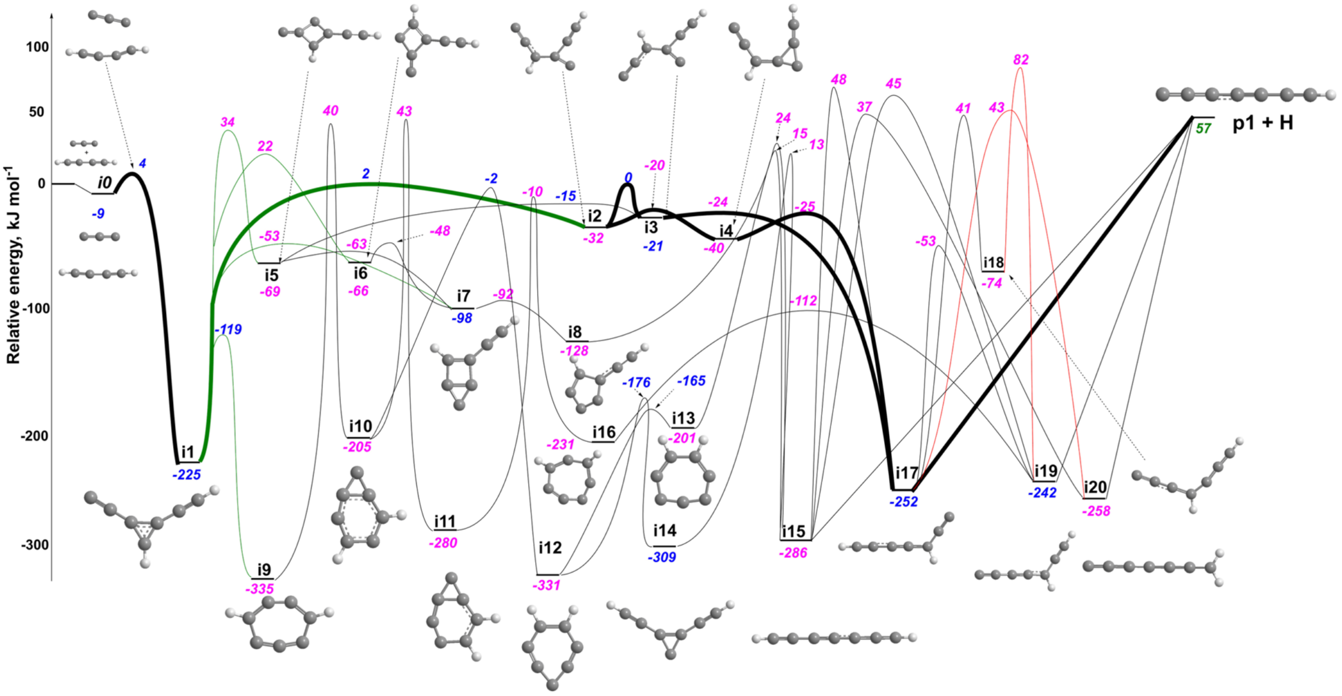

Figure 3. Potential energy surface for the bimolecular reaction of the tricarbon with diacetylene leading to *l*-C_7H plus the atomic hydrogen calculated at the different levels of theory: CCSD(T)-F12/cc-pVTZ-F12 (blue numbers), CASPT2(12,12)/cc-pVTZ (pink), and CASPT2(15,15)/cc-pVTZ (green). For a full list of energies calculated for each intermediate and transition state at different levels of theory refer to Table S1. Scanned potential energy profiles for the entrance channel and all exit channels confirming the barrierless character of H losses are illustrated in Figures S1−S5.

S1). However, despite this extensive repertoire of possible reaction pathways, the formation of only one product is feasible: the thermodynamically most stable C_7H isomer heptatriynylidyne (**p1**, $C_{\infty v}$, $X^2\Pi$) via an atomic hydrogen loss process. The second stable C_7H isomer 1,4-butadiynylcyclopropendiylidene (**p2**, C_{2v}, X^2B_2) lies about 100 kJ mol^{-1} above separated reactants.[78] Here, the low speed ratio of the tricarbon beam ($S = 3.8 \pm 0.8$) must be taken into account. In this case, it is beneficial to use a full distribution of collision energy instead of distribution of the most probable collision energy (E_C), which is 48 ± 17 kJ mol^{-1}. Considering the full distribution of collisional energies, the reaction energy Δ_rG can be calculated as 34 ± 25 kJ mol^{-1} overlapping the theoretically predicted reaction energy of the **p1** formation of 57 kJ mol^{-1}.

The calculations reveal that the reaction commences with the formation of an initial van der Waals complex (**i0**) submerged by 9 kJ mol^{-1} compared to the energy of the separated reactants (Figure 3). This complex may isomerize via the addition of the terminal atom of a tricarbon molecule to a carbon−carbon triple bond in diacetylene, forming the ring−chain carbene (**i1**) with a tricarbon ring that carries one atom from the tricarbon moiety and two atoms from the attacked triple bond (Table S1). For intermediate **i1**, all successive steps require the cleavage of one of the newly formed carbon−carbon single bonds within the cyclic C_3 moiety, which leads to **i2** via ring opening together with atomic hydrogen shift from diacetylene moiety, the incorporation of an additional carbon atom from the tricarbon moiety into the carbon ring resulting in **i5** or **i6**, the intermediate **i7** with a fused C_3 and C_4 ring whose formation requires rotation within the tricarbon moiety of the terminal carbon around the central one before the cycle opens and the formation of two new carbon rings ensues, and intermediate **i9** via ring closure that encloses all carbon atoms in the structure in the seven-membered ring. Further, **i2** or **i5** may form the carbene **i17** (1,2-heptadiene-4,6-diynylidene) via subsequent isomerization (**i2** → **i3** → **i17**; **i2** → **i4** → **i17**; **i5** → **i3** → **i17**). Isomers with similar structures **i5** and **i6** can undergo ring closure to **i7**, where two C_3 and C_4 rings can be merged into one C_5 ring via a small barrier accessing structure **i8**; the latter can further undergo a ring opening to the singlet biradical **i15** as one of the most stable acyclic C_7H_2 isomer on this PES. Both acyclic **i17** and **i15** can undergo atomic hydrogen loss yielding product **p1**. The PES includes interconnections between intermediates **i15**, **i17**, and **i19** and **i20** prior to their barrierless decomposition to **p1** via atomic hydrogen loss. However, the conversion of **i17** to **i19** through intermediate **i18** is closed since the energy of the **i18** → **i19** transition state lies substantially above the total available energy of this system. An additional low-lying pathway includes thermodynamically more stable cyclic C_7H_2 isomers (**i10**−**i14**) and commences from intermediate **i9** ultimately leading to **i15** or **i19** prior to unimolecular decomposition to **p1** + H. The first step requires a high barrier (375 kJ mol^{-1}) for a new carbon−carbon bond inside the C_7 ring leading to **i10** with fused C_3 and C_6 rings. From **i10**, the reaction can proceed to **i11** via an [1,2-H] atom shift, or alternatively, to **i12** regaining a C_7 ring. Starting from **i11**, the reaction may proceed to **i19** via an intermediate **i16**, while in another pathway, **i12** can access **i15** either via **i13** or **i14** structures. Which pathway will dominate this mechanism? The low-lying pathway that starts with the cyclic intermediate **i9** is more favored for the initial step from **i1**; however, the high barrier of 375 kJ mol^{-1} for the **i9** isomerization to **i10**, and further barriers of more than 200 kJ mol^{-1} makes this pathway less competitive compared to the reaction route involving **i2**, **i1** → **i2** → **i4** (**i3**) → **i17** → **p1** +

H. Thus, the most like intermediate decomposing to the final products is likely to be **i17**.

5. CONCLUSIONS

Exploiting the crossed molecular beam technique, we studied the reaction of tricarbon (C_3; $X^1\Sigma_g^+$) with diacetylene (butadiyne; HCCCCH; $X^1\Sigma_g^+$) at a collision energy of 47 ± 1 kJ mol^{-1}. The experimental data were augmented by electronic structure calculations to reveal the reaction mechanism. *Ab initio* calculations of the C_7H_2 PES demonstrate that this reaction starts from an initial van der Waals complex followed by the formation of the 2-(2-ethynyl-2-cyclopropen-1-ylidene)ethenylidene intermediate **i1** overcoming a barrier of 4 kJ mol^{-1}. Further, **i1** can rearrange to other C_7H_2 intermediates including **i2**, **i5**-**i7**, and **i9** by ring-opening and ring-closure processes and hydrogen atom migration. These intermediates can ultimately lead to several possible noncyclic C_7H_2 isomers **i15**, **i17**, **i19**, and **i20** before their barrierless unimolecular decomposition to the most stable linear C_7H isomer heptatriynylidyne (**p1**) in the endothermic process with the resulting reaction threshold of about 57 kJ mol^{-1}. No signal was detected at $m/z = 84$ (C_7^+) proving that the molecular hydrogen elimination channel is closed under our experimental conditions.

The above-mentioned reaction channels leading to hydrogen atom elimination, in general, are similar to what was found for the tricarbon reaction with acetylene (C_2H_2, $X^1\Sigma_g^+$),[35,79] except for the presence of distinct new low-lying pathway with a heptacarbon ring intermediate. In the theoretical study for C_3 + C_2H_2,[79] the authors predicted a dominating hydrogen elimination pathway to form the linear HCCCCC isomer with neglectable branching ratios for the molecular hydrogen channel plus pentacarbon (C_5) of 0.7% which was then verified by the crossed molecular beams experiment.[35] Absence of the signal of molecular hydrogen plus heptacarbon (C_7) channel at $m/z = 84$ (C_7^+) advocates similar behavior in the C_3 + C_4H_2 system. Here we can conclude that the behavior of tricarbon in reaction with acetylene and with the first member of the polyyne family is the same and leads to the formation of linear resonantly stabilized free radicals via reaction 3.

$$\begin{aligned} C_3(X^1\Sigma_g^+) + HC\equiv C-(C\equiv C)_{n=0,1}H(X^1\Sigma_g^+) \\ \rightarrow 1-C_{2n+5}H(X^2\Pi) + H(^2S_{1/2}) \end{aligned} \quad (3)$$

The significant energy threshold required for the tricarbon reaction implies that C_3 molecules can react with diacetylene (C_4H_2) to form linear resonantly stabilized free radical heptatriynylidyne (C_7H) in combustion flames and in extraterrestrial environments, such as circumstellar envelopes like IRC + 10216 and interstellar shock regions, where translational temperatures can reach up to a few thousand Kelvin. At the same time, this reaction is energetically prohibited in low-temperature environments, such as cold molecular clouds and in hydrocarbon-rich atmospheres of planets and their moons, such as Titan. This outcome may explain that so far heptatriynylidyne (C_7H) was detected only in the IRC + 10216[42] in the interstellar medium and remains elusive for the detection in cold molecular clouds like TMC-1.

■ ASSOCIATED CONTENT

Supporting Information

The Supporting Information is available free of charge at https://pubs.acs.org/doi/10.1021/acs.jpca.5c01330.

> Relative energies (E_{rel}) calculated at the different levels of theory, total spin operator expectation values (spin contamination; $\langle S_{UHF}^2\rangle$), and T1 diagnostic values of intermediates and transition states on the potential energy surface; potential energy profile for the entrance reaction; scanned relaxed potential energy profile for exit channels; optimized Cartesian coordinates and vibrational frequencies for all intermediates, transition states, reactants, and products involved in the C_3 + C_4H_2 reactions at the ωB97X-D/6-311G(d,p) level; scanned potential energy profiles for the entrance channel and all exit channels confirming the barrierless character of H losses; and the unsuccessful fit of the experimental LAD and TOFs with a reaction cross section proportional to $E_C^{-(1/3)}$ (PDF)

■ AUTHOR INFORMATION

Corresponding Authors

Alexander M. Mebel − *Department of Chemistry and Biochemistry, Florida International University, Miami, Florida 33199, United States*; orcid.org/0000-0002-7233-3133; Email: mebela@fiu.edu
Ralf I. Kaiser − *Department of Chemistry, University of Hawai'i at Manoa, Honolulu, Hawaii 96822, United States*; orcid.org/0000-0002-7233-7206; Email: ralfk@hawaii.edu

Authors

Iakov A. Medvedkov − *Department of Chemistry, University of Hawai'i at Manoa, Honolulu, Hawaii 96822, United States*; orcid.org/0000-0003-0672-2090
Anatoliy A. Nikolayev − *Samara National Research University, Samara 443086, Russia*
Zhenghai Yang − *Department of Chemistry, University of Hawai'i at Manoa, Honolulu, Hawaii 96822, United States*
Shane J. Goettl − *Department of Chemistry, University of Hawai'i at Manoa, Honolulu, Hawaii 96822, United States*; orcid.org/0000-0003-1796-5725
Alina A. Kuznetsova − *Samara National Research University, Samara 443086, Russia*
André K. Eckhardt − *Lehrstuhl für Organische Chemie II, Ruhr-Universität Bochum, 44801 Bochum, Germany*; orcid.org/0000-0003-1029-9272

Complete contact information is available at: https://pubs.acs.org/10.1021/acs.jpca.5c01330

Author Contributions

The manuscript was written through contributions of all authors. All authors have given approval to the final version of the manuscript.

Notes

The authors declare no competing financial interest.

■ ACKNOWLEDGMENTS

The experimental studies at the University of Hawai'i at Manoa were supported by the US Department of Energy, Basic Energy Sciences (DE-FG02-03ER15411). The chemical synthesis was supported by the Deutsche Forschungsgemeinschaft (DFG, German Research Foundation) under Germany's Excellence Strategy−EXC-2033-390677874−RESOLV and the Fonds der Chemischen Industrie (Liebig Fellowship to A.K.E.).

■ REFERENCES

(1) Frenklach, M.; Mebel, A. M. On the Mechanism of Soot Nucleation. *Phys. Chem. Chem. Phys.* **2020**, *22* (9), 5314−5331.

(2) Frenklach, M. Reaction Mechanism of Soot Formation in Flames. *Phys. Chem. Chem. Phys.* **2002**, *4* (11), 2028−2037.

(3) Marinov, N. M.; Pitz, W. J.; Westbrook, C. K.; Castaldi, M. J.; Senkan, S. M. Modeling of Aromatic and Polycyclic Aromatic Hydrocarbon Formation in Premixed Methane and Ethane Flames. *Combust. Sci. Technol.* **1996**, *116*−*117* (1−6), 211−287.

(4) Galimova, G. R.; Medvedkov, I. A.; Mebel, A. M. The Role of Methylaryl Radicals in the Growth of Polycyclic Aromatic Hydrocarbons: The Formation of Five-Membered Rings. *J. Phys. Chem. A* **2022**, *126* (7), 1233−1244.

(5) Kaiser, R. I.; Stranges, D.; Bevsek, H. M.; Lee, Y. T.; Suits, A. G. Crossed-Beam Reaction of Carbon Atoms with Hydrocarbon Molecules. IV. Chemical Dynamics of Methylpropargyl Radical Formation, C_4H_5, from Reaction of $C(^3P_j)$ with Propylene, C_3H_6 (X^1A). *J. Chem. Phys.* **1997**, *106* (12), 4945−4953.

(6) Medvedkov, I. A.; Yang, Z.; Nikolayev, A. A.; Goettl, S. J.; Eckhardt, A. K.; Mebel, A. M.; Kaiser, R. I. Binding the Power of Cycloaddition and Cross-Coupling in a Single Mechanism: An Unexpected Bending Journey to Radical Chemistry of Butadiynyl with Conjugated Dienes. *J. Phys. Chem. Lett.* **2025**, *16* (2), 658−666.

(7) Kaiser, R. I.; Hansen, N. An Aromatic Universe − A Physical Chemistry Perspective. *J. Phys. Chem. A* **2021**, *125* (18), 3826−3840.

(8) Kaiser, R. I. Experimental Investigation on the Formation of Carbon-Bearing Molecules in the Interstellar Medium via Neutral−Neutral Reactions. *Chem. Rev.* **2002**, *102* (5), 1309−1358.

(9) Kaiser, R. I.; Mebel, A. M. The Reactivity of Ground-State Carbon Atoms with Unsaturated Hydrocarbons in Combustion Flames and in the Interstellar Medium. *Int. Rev. Phys. Chem.* **2002**, *21* (2), 307−356.

(10) Gu, X.; Kaiser, R. I.; Mebel, A. M. Chemistry of Energetically Activated Cumulenes—From Allene (H_2CCCH_2) to Hexapentaene ($H_2CCCCCCH_2$). *ChemPhysChem* **2008**, *9* (3), 350−369.

(11) Mebel, A. M.; Kaiser, R. I. Formation of Resonantly Stabilised Free Radicals via the Reactions of Atomic Carbon, Dicarbon, and Tricarbon with Unsaturated Hydrocarbons: Theory and Crossed Molecular Beams Experiments. *Int. Rev. Phys. Chem.* **2015**, *34* (4), 461−514.

(12) Kaiser, R. I.; Balucani, N. Astrobiology − the Final Frontier in Chemical Reaction Dynamics. *Int. J. Astrobiol.* **2002**, *1* (1), 15−23.

(13) Frenklach, M.; Clary, D. W.; Gardiner, W. C.; Stein, S. E. Detailed Kinetic Modeling of Soot Formation in Shock-Tube Pyrolysis of Acetylene. *Symp. (Int.) Combust.* **1985**, *20* (1), 887−901.

(14) Kaiser, R. I.; Maksyutenko, P.; Ennis, C.; Zhang, F.; Gu, X.; Krishtal, S. P.; Mebel, A. M.; Kostko, O.; Ahmed, M. Untangling the Chemical Evolution of Titan's Atmosphere and Surface−from Homogeneous to Heterogeneous Chemistry. *Faraday Discuss.* **2010**, *147*, 429−478.

(15) Shiomi, T.; Nagai, H.; Kato, K.; Hiramatsu, M.; Nawata, M. Detection of C_2 Radicals in Low-Pressure Inductively Coupled Plasma Source for Diamond Chemical Vapor Deposition. *Diamond Relat. Mater.* **2001**, *10* (3), 388−392.

(16) Kaiser, R. I.; Stranges, D.; Lee, Y. T.; Suits, A. G. Neutral-Neutral Reactions in the Interstellar Medium. I. Formation of Carbon Hydride Radicals via Reaction of Carbon Atoms with Unsaturated Hydrocarbons. *Astrophys. J.* **1997**, *477* (2), 982.

(17) Gu, X.; Guo, Y.; Zhang, F.; Mebel, A. M.; Kaiser, R. I. Reaction Dynamics of Carbon-Bearing Radicals in Circumstellar Envelopes of Carbon Stars. *Faraday Discuss.* **2006**, *133*, 245.

(18) Kaiser, R. I.; Le, T. N.; Nguyen, T. L.; Mebel, A. M.; Balucani, N.; Lee, Y. T.; Stahl, F.; Schleyer, P. v R.; Iii, H. F. S. A Combined Crossed Molecular Beam and Ab Initio Investigation of C_2 and C_3 Elementary Reactions with Unsaturated Hydrocarbons—Pathways to Hydrogen Deficient Hydrocarbon Radicals in Combustion Flames. *Faraday Discuss.* **2002**, *119* (0), 51−66.

(19) Gaydon, A. G. *The Spectroscopy of Flames*; Springer Netherlands: Dordrecht, 1974.

(20) Hinkle, K. W.; Keady, J. J.; Bernath, P. F. Detection of C_3 in the Circumstellar Shell of IRC + 10216. *Science* **1988**, *241* (4871), 1319−1322.

(21) Geppert, W. D.; Naulin, C.; Costes, M.; Capozza, G.; Cartechini, L.; Casavecchia, P.; Gualberto Volpi, G. Combined Crossed-Beam Studies of $C(^3P_j) + C_2H_4 \rightarrow C_3H_3 + H$ Reaction Dynamics between 0.49 and 30.8 kJ Mol^{-1}. *J. Chem. Phys.* **2003**, *119* (20), 10607−10617.

(22) Balucani, N.; Leonori, F.; Petrucci, R.; Hickson, K. M.; Casavecchia, P. Crossed Molecular Beam Studies of $C(^3P,^1D)$ and $C_2(X^1\Sigma_g^+,a^3\Pi_u)$ Reactions with Acetylene. *Phys. Scr.* **2008**, *78* (5), No. 058117.

(23) Parker, D. S. N.; Zhang, F.; Kim, Y. S.; Kaiser, R. I.; Mebel, A. M. On the Formation of Resonantly Stabilized C_5H_3 Radicals—A Crossed Beam and Ab Initio Study of the Reaction of Ground State Carbon Atoms with Vinylacetylene. *J. Phys. Chem. A* **2011**, *115* (5), 593−601.

(24) Kaiser, R. I.; Mebel, A. M.; Chang, A. H. H.; Lin, S. H.; Lee, Y. T. Crossed-Beam Reaction of Carbon Atoms with Hydrocarbon Molecules. V. Chemical Dynamics of n-C_4H_3 Formation from Reaction of $C(^3P_j)$ with Allene, $H_2CCCH_2(X\,^1A_1)$. *J. Chem. Phys.* **1999**, *110* (21), 10330−10344.

(25) Thomas, A. M.; Lucas, M.; Zhao, L.; Liddiard, J.; Kaiser, R. I.; Mebel, A. M. A Combined Crossed Molecular Beams and Computational Study on the Formation of Distinct Resonantly Stabilized C_5H_3 Radicals *via* Chemically Activated C_5H_4 and C_6H_6 Intermediates. *Phys. Chem. Chem. Phys.* **2018**, *20* (16), 10906−10925.

(26) Dangi, B. B.; Maity, S.; Kaiser, R. I.; Mebel, A. M. A Combined Crossed Beam and Ab Initio Investigation of the Gas Phase Reaction of Dicarbon Molecules (C_2; $X^1\Sigma_g^+$/a $^3\Pi_u$) with Propene (C_3H_6; X^1A'): Identification of the Resonantly Stabilized Free Radicals 1- and 3-Vinylpropargyl. *J. Phys. Chem. A* **2013**, *117* (46), 11783−11793.

(27) Zhang, F.; Kim, S.; Kaiser, R. I.; Mebel, A. M. Formation of the 1,3,5-Hexatriynyl Radical ($C_6H(X^2\Pi)$) via the Crossed Beams Reaction of Dicarbon ($C_2(X^1\Sigma_g^+/a^3\Pi_u)$), with Diacetylene ($C_4H_2(X^1\Sigma_g^+)$). *J. Phys. Chem. A* **2009**, *113* (7), 1210−1217.

(28) Kaiser, R. I.; Goswami, M.; Maksyutenko, P.; Zhang, F.; Kim, Y. S.; Landera, A.; Mebel, A. M. A Crossed Molecular Beams and Ab Initio Study on the Formation of C_6H_3 Radicals. An Interface between Resonantly Stabilized and Aromatic Radicals. *J. Phys. Chem. A* **2011**, *115* (37), 10251−10258.

(29) Zhang, F.; Jones, B.; Maksyutenko, P.; Kaiser, R. I.; Chin, C.; Kislov, V. V.; Mebel, A. M. Formation of the Phenyl Radical [$C_6H_5(X^2A_1)$] under Single Collision Conditions: A Crossed Molecular Beam and Ab Initio Study. *J. Am. Chem. Soc.* **2010**, *132* (8), 2672−2683.

(30) Parker, D. S. N.; Maity, S.; Dangi, B. B.; Kaiser, R. I.; Landera, A.; Mebel, A. M. Understanding the Chemical Dynamics of the Reactions of Dicarbon with 1-Butyne, 2-Butyne, and 1,2-Butadiene − toward the Formation of Resonantly Stabilized Free Radicals. *Phys. Chem. Chem. Phys.* **2014**, *16* (24), 12150−12163.

(31) Dangi, B. B.; Parker, D. S. N.; Yang, T.; Kaiser, R. I.; Mebel, A. M. Gas-Phase Synthesis of the Benzyl Radical ($C_6H_5CH_2$). *Angew. Chem., Int. Ed.* **2014**, *53* (18), 4608−4613.

(32) Dangi, B. B.; Parker, D. S. N.; Kaiser, R. I.; Belisario-Lara, D.; Mebel, A. M. An Experimental and Theoretical Investigation of the Formation of C_7H_7 Isomers in the Bimolecular Reaction of Dicarbon Molecules with 1,3-Pentadiene. *Chem. Phys. Lett.* **2014**, *607*, 92−99.

(33) Balucani, N.; Mebel, A. M.; Lee, Y. T.; Kaiser, R. I. A Combined Crossed Molecular Beam and Ab Initio Study of the Reactions $C_2(X\Sigma_g^+,\ a^3\Pi_u) + C_2H_4 \rightarrow$ n-$C_4H_3(XA')$ + $H(^2S^{1/2})$. *J. Phys. Chem. A* **2001**, *105* (43), 9813−9818.

(34) Kaiser, R. I.; Balucani, N.; Charkin, D. O.; Mebel, A. M. A Crossed Beam and Ab Initio Study of the $C_2(X^1\sum_g^+ /a^3\prod_u)$ + $C_2H_2(X^1\sum_g^+)$ Reactions. *Chem. Phys. Lett.* **2003**, *382* (1), 112−119.

(35) Gu, X.; Guo, Y.; Mebel, A. M.; Kaiser, R. I. A Crossed Beam Investigation of the Reactions of Tricarbon Molecules, $C_3(X^1\sum_g^+)$, with Acetylene, $C_2H_2(X_1\sum_g^+)$, Ethylene, $C_2H_4(X_1A_g)$, and Benzene, $C_6H_6(X^1A_{1g})$. *Chem. Phys. Lett.* **2007**, *449* (1−3), 44−52.

(36) Guo, Y.; Gu, X.; Zhang, F.; Mebel, A. M.; Kaiser, R. I. A Crossed Molecular Beam Study on the Formation of Hexenediynyl Radicals ($H_2CCCCCCH$; C_6H_3 ($X\ ^2A'$)) via Reactions of Tricarbon Molecules, C_3 ($X^1\sum_g^+$), with Allene (H $_2CCCH_2$; X^1A_1) and Methylacetylene (CH_3CCH; X^1A_1). *Phys. Chem. Chem. Phys.* **2007**, *9* (16), 1972−1979.

(37) McGuire, B. A. 2021 Census of Interstellar, Circumstellar, Extragalactic, Protoplanetary Disk, and Exoplanetary Molecules. *ApJS* **2022**, *259* (2), 30.

(38) Medvedkov, I. A.; A Nikolayev, A.; Yang, Z.; J Goettl, S.; M Mebel, A.; I Kaiser, R. Elucidating the Chemical Dynamics of the Elementary Reactions of the 1-Propynyl Radical (CH_3CC; X^2A_1) with 2-Methylpropene ($(CH_3)_2CCH_2$; X_1A^1). *Phys. Chem. Chem. Phys.* **2024**, *26* (7), 6448−6457.

(39) Zhang, F.; Kim, Y. S.; Zhou, L.; Chang, A. H. H.; Kaiser, R. I. A Crossed Molecular Beam Study on the Synthesis of the Interstellar 2,4-Pentadiynylidyne Radical (HCCCCC). *J. Chem. Phys.* **2008**, *129* (13), No. 134313.

(40) Travers, M. J.; McCarthy, M. C.; Gottlieb, C. A.; Thaddeus, P. Laboratory Detection of the C_7H Radical. *Astrophys. J.* **1996**, *465* (1), L77.

(41) McCarthy, M. C.; Travers, M. J.; Kovács, A.; Gottlieb, C. A.; Thaddeus, P. Eight New Carbon Chain Molecules. *Astrophys. J. Suppl. Ser.* **1997**, *113* (1), 105.

(42) Guelin, M.; Cernicharo, J.; Travers, M. J.; McCarthy, M. C.; Gottlieb, C. A.; Thaddeus, P.; Ohishi, M.; Saito, S.; Yamamoto, S. Detection of a New Linear Carbon Chain Radical: C_7_H. *Astron. Astrophys.* **1997**, *317*, L1−L4.

(43) Bell, M. B.; Feldman, P. A.; Watson, J. K. G.; McCarthy, M. C.; Travers, M. J.; Gottlieb, C. A.; Thaddeus, P. Observations of Long CnH Molecules in the Dust Cloud TMC-1. *Astrophys. J.* **1999**, *518* (2), 740.

(44) Guo, Y.; Gu, X.; Kawamura, E.; Kaiser, R. I. Design of a Modular and Versatile Interlock System for Ultrahigh Vacuum Machines: A Crossed Molecular Beam Setup as a Case Study. *Rev. Sci. Instrum.* **2006**, *77* (3), No. 034701.

(45) Medvedkov, I. A.; Nikolayev, A. A.; He, C.; Yang, Z.; Mebel, A. M.; Kaiser, R. I. One Collision—Two Substituents: Gas-Phase Preparation of Xylenes under Single-Collision Conditions. *Angew. Chem., Int. Ed.* **2024**, *63* (5), No. e202315147.

(46) Gu, X.; Guo, Y.; Kawamura, E.; Kaiser, R. I. Characteristics and Diagnostics of an Ultrahigh Vacuum Compatible Laser Ablation Source for Crossed Molecular Beam Experiments. *J. Vac. Sci. Technol. A* **2006**, *24* (3), 505−511.

(47) Medvedkov, I. A.; Nikolayev, A. A.; Goettl, S. J.; Yang, Z.; Mebel, A. M.; Kaiser, R. I. Experimental and Theoretical Study of the Sn−O Bond Formation between Atomic Tin and Molecular Oxygen. *Phys. Chem. Chem. Phys.* **2024**, *26* (43), 27763−27771.

(48) Zhou, L.; Kaiser, R. I.; Tokunaga, A. T. Infrared Spectroscopy of Crystalline and Amorphous Diacetylene (C_4H_2) and Implications for Titan's Atmospheric Composition. *Planet. Space Sci.* **2009**, *57* (7), 830−835.

(49) Jones, A. V.; Herzberg, G. Infra-Red and Raman Spectra of Diacetylene. *Proc. R. Soc. Lond., Ser. A* **1997**, *211* (1105), 285−295.

(50) Okabe, H. Photochemistry of Acetylene at 1470 Å. *J. Chem. Phys.* **1981**, *75* (6), 2772−2778.

(51) Lee, Y. T. Molecular Beam Studies of Elementary Chemical Processes. *Science* **1987**, *236* (4803), 793−798.

(52) Herschbach, D. R. Molecular Dynamics of Elementary Chemical Reactions (Nobel Lecture). *Angew. Chem., Int. Ed.* **1987**, *26* (12), 1221−1243.

(53) Daly, N. R. Scintillation Type Mass Spectrometer Ion Detector. *Rev. Sci. Instrum.* **1960**, *31* (3), 264−267.

(54) Vernon, M. F. Molecular Beam Scattering, Ph.D. Dissertation; University of California: Berkeley, CA, 1983.

(55) Weiss, P. S. Reaction Dynamics of Electronically Excited Alkali Atoms with Simple Molecules, Ph.D. Dissertation; University of California: Berkeley, CA, 1986.

(56) Levine, R. D. *Molecular Reaction Dynamics*; Cambridge University Press: Cambridge, U.K., 2005.

(57) Steinfeld, J. I.; Francisco, J. S.; Hase, W. L. *Chemical Kinetics and Dynamics*, 2nd ed.; Pearson: Upper Saddle River, N.J, 1998.

(58) Chai, J.-D.; Head-Gordon, M. Long-Range Corrected Hybrid Density Functionals with Damped Atom−Atom Dispersion Corrections. *Phys. Chem. Chem. Phys.* **2008**, *10* (44), 6615−6620.

(59) Krishnan, R.; Binkley, J. S.; Seeger, R.; Pople, J. A. Self-Consistent Molecular Orbital Methods. XX. A Basis Set for Correlated Wave Functions. *J. Chem. Phys.* **1980**, *72* (1), 650−654.

(60) Frisch, M. J.; Trucks, G. W.; Schlegel, H. B.; Scuseria, G. E.; Robb, M. A.; Cheeseman, J. R.; Scalmani, G.; Barone, V.; Mennucci, B.; Petersson, G. A.et al. *Gaussian 09*; Gaussian Inc.: Wallingford, CT, 2009.

(61) Hratchian, H. P.; Schlegel, H. B. Accurate Reaction Paths Using a Hessian Based Predictor−Corrector Integrator. *J. Chem. Phys.* **2004**, *120* (21), 9918−9924.

(62) Adler, T. B.; Knizia, G.; Werner, H.-J. A Simple and Efficient CCSD(T)-F12 Approximation. *J. Chem. Phys.* **2007**, *127* (22), No. 221106.

(63) Knizia, G.; Adler, T. B.; Werner, H.-J. Simplified CCSD(T)-F12 Methods: Theory and Benchmarks. *J. Chem. Phys.* **2009**, *130* (5), No. 054104.

(64) Dunning, T. H., Jr. Gaussian Basis Sets for Use in Correlated Molecular Calculations. I. The Atoms Boron through Neon and Hydrogen. *J. Chem. Phys.* **1989**, *90* (2), 1007−1023.

(65) Werner, H.-J.; Knowles, P. J.; Lindh, R.; Manby, F. R.; Schütz, M.; Celani, P.; Korona, T.; Rauhut, G.; Amos, R. D.; Bernhardsson, A. MOLPRO, Revision 2015.1, A Package of Ab Initio Programs; University of Cardiff: Cardiff, UK, 2015.

(66) Celani, P.; Werner, H.-J. Multireference Perturbation Theory for Large Restricted and Selected Active Space Reference Wave Functions. *J. Chem. Phys.* **2000**, *112* (13), 5546−5557.

(67) Shiozaki, T.; Győrffy, W.; Celani, P.; Werner, H.-J. Communication: Extended Multi-State Complete Active Space Second-Order Perturbation Theory: Energy and Nuclear Gradients. *J. Chem. Phys.* **2011**, *135* (8), No. 081106.

(68) Werner, H.-J.; Knowles, P. J A Second Order Multiconfiguration SCF Procedure with Optimum Convergence. *J. Chem. Phys.* **1985**, *82* (11), 5053−5063.

(69) Knowles, P. J.; Werner, H.-J. An Efficient Second-Order MC SCF Method for Long Configuration Expansions. *Chem. Phys. Lett.* **1985**, *115* (3), 259−267.

(70) Miller, J. A.; Klippenstein, S. J.; Georgievskii, Y.; Harding, L. B.; Allen, W. D.; Simmonett, A. C. Reactions between Resonance-Stabilized Radicals: Propargyl + Allyl. *J. Phys. Chem. A* **2010**, *114* (14), 4881−4890.

(71) Matsugi, A.; Miyoshi, A. Computational Study on the Recombination Reaction between Benzyl and Propargyl Radicals. *Int. J. Chem. Kinet.* **2012**, *44* (3), 206−218.

(72) Zhang, J.; Valeev, E. F. Prediction of Reaction Barriers and Thermochemical Properties with Explicitly Correlated Coupled-Cluster Methods: A Basis Set Assessment. *J. Chem. Theory Comput.* **2012**, *8* (9), 3175−3186.

(73) Kaiser, R. I.; Mebel, A. M. On the Formation of Polyacetylenes and Cyanopolyacetylenes in Titan's Atmosphere and Their Role in Astrobiology. *Chem. Soc. Rev.* **2012**, *41* (16), 5490.

(74) Lee, Y. T. Molecular Beam Studies of Elementary Chemical Processes(Nobel Lecture). *Angew. Chem., Int. Ed.* **1987**, *26* (10), 939−951.

(75) Brouard, M.; Vallance, C. *Tutorials in Molecular Reaction Dynamics*, 1st ed.; Royal Society of Chemistry: La Vergne, 2010.

(76) Taylor, E. H.; Datz, S. Study of Chemical Reaction Mechanisms with Molecular Beams. The Reaction of K with HBr. *J. Chem. Phys.* **1955**, *23* (9), 1711−1718.

(77) Miller, W. B.; Safron, S. A.; Herschbach, D. R. Exchange Reactions of Alkali Atoms with Alkali Halides: A Collision Complex Mechanism. *Discuss. Faraday Soc.* **1967**, *44*, 108.

(78) Sun, B. J.; Huang, C. H.; Tsai, M. F.; Sun, H. L.; Gao, L. G.; Wang, Y. S.; Yeh, Y. Y.; Shih, Y. H.; Sia, Z. F.; Chen, P. H.; et al. Synthesis of Interstellar 1,3,5-Heptatriynylidyne, $C_7H(X^2\Pi)$, via the Neutral-Neutral Reaction of Ground State Carbon Atom, $C(^3P)$, with Triacetylene, HC_6H $(X^1\sum_g{}^+)$. *J. Chem. Phys.* **2009**, *131* (10), No. 104305.

(79) Mebel, A. M.; Kim, G.-S.; Kislov, V. V.; Kaiser, R. I. The Reaction of Tricarbon with Acetylene: An Ab Initio/RRKM Study of the Potential Energy Surface and Product Branching Ratios. *J. Phys. Chem. A* **2007**, *111* (29), 6704−6712.